



On the estimate of the FRFs from operational data

Giuliano Coppotelli

Dipartimento di Ingegneria Aerospaziale e Astronautica, Università degli Studi di Roma "La Sapienza", Via Eudossiana, 16, 00184 Rome, Italy

ARTICLE INFO

Article history:

Received 13 December 2007

Received in revised form

15 February 2008

Accepted 5 May 2008

Available online 17 May 2008

PACS:

43.40

62.30.+d

Keywords:

Output only analysis

Experimental modal analysis

Structural dynamics

ABSTRACT

In this paper, the effects of different mass loadings required for the estimation of the frequency response functions, FRFs, from data gained by the emerging technique of operational modal testing, is proposed. This technique allows the evaluation of the natural frequencies, mode shapes and damping ratios from operational data achieved from a first session of tests, then the scaling factors are derived from a further experimental investigation. The approach is based on the sensitivity of the eigenproperties to structural modifications, such as the mass and stiffness distribution. It is shown that the generalized modal parameters could be derived by the measurements of the natural frequency shifts due to a controlled mass variation in the structure, assuming negligible changes in the mode shapes. Such generalized modal parameters are finally used to estimate the FRFs. This mode shape scaling technique, together with the investigation of the effects of the mass positioning on the uncertainties in the estimates of the scaling factors will be experimentally investigated on simple aerospace structures.

© 2008 Elsevier Ltd. All rights reserved.

1. Introduction

The dynamic signature of structures is generally identified by the “standard” experimental modal analysis (EMA) approaches that require the measure of both the input loadings and the corresponding structural responses, Ref. [1]. Although the high accuracy in the estimate of the modal model these approaches have gained, in recent years many research groups have focused their activities on those methods capable to identify such modal parameters using the ambient excitation and measuring only the responses of the structure. These activities led to the development of the so-called ambient, or operational, or output only modal analysis, Refs. [2–4]. With respect to the traditional EMA techniques, the test setup for the output only modal analysis will consider only the measurements of the responses of the system, resulting then an easier way for characterizing the dynamic behavior of the structure. In addition, this approach could identify the dynamic properties of the system in real operative conditions where the boundary conditions are, in general, substantially different from those simulated in the modal tests performed in the labs, or even unknown. Also, these output only approaches are giving better and more reliable results in cases where the actual loading and operating conditions are important for the structural response, Ref. [5], or for those tests where the loadings are roughly replicated during the traditional spectral analysis. Moreover, this capability to extract the modal parameters of the system under the real operating conditions represents a great advantage of these techniques from the industrial point of view since their reliability and the low costs associated to the whole test phase. Moreover, this approach could be used to improve the modal models measured in the laboratory to better reflect the actual behavior of the system under the operational situation, to update the numerical model of the system, and finally, to monitor the integrity of the structure during its operational life, Ref. [3]. Nevertheless, these techniques need further improvements in many crucial topics such as closed

E-mail address: giuliano.coppotelli@uniroma1.it

URL: <http://www.diaa.uniroma1.it/docenti/g.coppotelli/index.html>

mode identification, modal damping estimation, and mode shape scaling, Ref. [6]. In this paper, the generalized parameters, or scaling factors, are achieved by an experimental/numerical procedure based on the work done in Ref. [5], and in Ref. [7], that—in turn—could be originated, for some items, from the pioneer work presented in Ref. [8]. The core of the approach is the sensitivity of the modal parameters to changes of the mass and the stiffness properties of the structure. If such structural modifications have no influences on the mode shapes, then the unknown scaling factors are estimated from the knowledge of the structural perturbation itself and from the measurements of the corresponding eigenfrequency shifts. This is an appealing results since the aim of the additional test will be the estimate of the natural frequencies only, speeding up the entire procedure. Although both mass and stiffness perturbations could be used in order to produce the eigenfrequency shifts, changing the mass distribution is easier from the practical point of view. First, the unscaled modal mode shapes, natural frequencies, and damping ratios are estimated using both the frequency domain decomposition FDD, technique, Ref. [9], and the logarithmic decrement techniques. Then, a second experimental test is performed to estimate the generalized parameters from the measure of the eigenfrequency shifts induced by a known mass change of the structure. The generalized masses associated to the eigenmodes considered in the experimental analysis are identified, and then the residues needed to estimate the frequency response function (FRF) of the system can be achieved. This response model could be finally used to improve the numerical representation of the structure, i.e., Finite Element model, as reported in Ref. [10], where the FRFs were used for correlation and structural updating problems. The experiences gained by the author during the different output only investigations on simple structures, Refs. [11–13], are here reported to validate the whole procedure to estimate the FRFs from operational data. Furthermore, the effects of mass loading and positioning on the evaluation of the scaling factors are also analyzed.

2. Theoretical basis

2.1. Background on FDD

The aim of the developed procedure is the estimate of the modal parameters by using output only data. In this approach, the analysis of the response data is made in the frequency domain using the well-known FDD method. In this section, the key points of this method will be briefly summarized. The readers should refer to Ref. [9] for further details. Considering the time responses of the vibrating structure measured at N_o measurement points, $x_i(t), i = 1, \dots, N_o$, the auto, $R_{x_i x_i}(\tau)$, and cross, $R_{x_i x_j}(\tau)$, correlation functions are defined as follows:

$$R_{x_i x_i}(\tau) = E[x_i(t), x_i(t + \tau)] = \lim_{T \rightarrow \infty} \frac{1}{T} \int_{-T/2}^{+T/2} x_i(t)x_i(t + \tau) dt \tag{1}$$

$$R_{x_i x_j}(\tau) = E[x_i(t), x_j(t + \tau)] = \lim_{T \rightarrow \infty} \frac{1}{T} \int_{-T/2}^{+T/2} x_i(t)x_j(t + \tau) dt \tag{2}$$

in which $E[\cdot]$ is the expected value operator. These correlation functions of the time shift τ not only allow one to completely describe nondeterministic signals, under the hypothesis of Gaussian stationary, ergodic with zero mean value signals, $x_i(t)$, but also the auto and cross spectral density functions could be evaluated from the Wiener–Khinchine relations, Ref. [14]:

$$G_{x_i x_i}(\omega) = \int_{-\infty}^{+\infty} R_{x_i x_i}(\tau)e^{-j\omega\tau} d\tau, \quad G_{x_i x_j}(\omega) = \int_{-\infty}^{+\infty} R_{x_i x_j}(\tau)e^{-j\omega\tau} d\tau \tag{3}$$

The spectral density matrix of the response signals, $G_{xx}(\omega) \in \mathbb{C}^{N_o \times N_o}$, is then computed as follows:

$$G_{xx}(\omega) = \begin{pmatrix} G_{x_1 x_1}(\omega) & G_{x_1 x_2}(\omega) & \cdots & G_{x_1 x_{N_o}}(\omega) \\ G_{x_2 x_1}(\omega) & \cdots & \cdots & \cdots \\ \vdots & \vdots & \vdots & \vdots \\ G_{x_{N_o} x_1}(\omega) & G_{x_{N_o} x_2}(\omega) & \cdots & G_{x_{N_o} x_{N_o}}(\omega) \end{pmatrix} \tag{4}$$

This spectral density matrix could be expressed in terms of the FRF matrix of the system, $H(\omega) \in \mathbb{C}^{N_o \times N_i}$ with N_i the number of the input loadings, by the following relation:

$$G_{xx}(\omega) = H(\omega)G_{ff}(\omega)H^H(\omega) \tag{5}$$

where $G_{ff}(\omega) \in \mathbb{C}^{N_i \times N_i}$ is the spectral density matrix of the input. Introducing the modal properties of the dynamic system, it is possible to relate the FRF matrix to:

- the modal vector matrix, formed by N mode shapes, $V \in \mathbb{C}^{N_o \times 2N}$, i.e., $V = [\psi^{(1)}, \dots, \psi^{(N)}, \psi^{(1)*}, \dots, \psi^{(N)*}]$ where the superscript * denote complex conjugate,
- the diagonal matrix, $A \in \mathbb{C}^{2N \times 2N}$, of the system poles, $\lambda_k = \sigma_k + j\omega_{dk}$, where σ_k and ω_{dk} are the k -th damping factor and damped natural frequency, respectively, and
- the modal participation factor matrix, $L \in \mathbb{C}^{2N \times N_i}$.

As reported in Ref. [15], this relationship could be written as

$$H(\omega) = V(j\omega I - A)^{-1}L \quad (6)$$

Combining the previous Eqs. (6) and (5), it is possible to write

$$G_{xx}(\omega) = V(j\omega I - A)^{-1}L G_{ff}(\omega) L^H (j\omega I - A)^{-*} V^H \quad (7)$$

where H and $^{-*}$ represent the hermitian and complex conjugate of the matrix inversion operations, respectively. This equation could be further simplified if the hypotheses of uncorrelated white noise input loadings, at least in the frequency band of interest, i.e., $G_{ff}(\omega) = \text{const.}$, and low damping ratios, with well separated modes, are considered. In this case, by applying the Heaviside partial fraction theorem, Eq. (7) could be rewritten as

$$G_{xx}(\omega) = V(j\omega I - A)^{-1} D V^H \quad (8)$$

where the resulting projection of the unknown input level on the modal base forms the diagonal matrix, $D \in \mathbb{C}^{2N \times 2N}$, of scalar constant d_k , Ref. [9]. If a limited number of modes, M , will significantly contribute to the formation of the output response spectral matrix, at the frequency ω , then the previous equation could be rewritten so that the mode contribution is highlighted, Refs. [2,9]:

$$G_{xx}(\omega) = \sum_{k=1}^M \frac{d_k \psi^{(k)} \psi^{(k)\top}}{j\omega - \lambda_k} + \frac{d_k^* \psi^{(k)*} \psi^{(k)H}}{j\omega - \lambda_k^*} \quad (9)$$

Recalling that the structure behaves as a single degree of freedom (SDOF) system around the peak of resonance, i.e., the structure is characterized by low damping ratios and well separated mode shapes, then only the k -th mode will dominate the right-hand side of Eq. (9), when evaluated at a frequency equal to one of the k -th eigenfrequency ω_{nk} ($k = 1, \dots, M$). Therefore, at resonance, the power spectral density matrix of the responses is related to the modal model as

$$G_{xx}(\omega_{nk}) = \frac{d_k \psi^{(k)} \psi^{(k)\top}}{j\omega_{nk} - \lambda_k} + \frac{d_k^* \psi^{(k)*} \psi^{(k)H}}{j\omega_{nk} - \lambda_k^*} \quad (10)$$

The previous relations must consider digital time series with proper concern for the quantization and aliasing problems. Assuming the digital data formed by N_s sampling values, the spectral density matrix will be computed on a FFT-based procedure and it will be defined at discrete frequency lines ω_i , ($i = 0, 1, 2, \dots, N_s/2$). For each of the available frequency lines, it is possible to have a spectral representation of the $G_{xx}(\omega_i)$ matrix through the singular value decomposition (SVD) algorithm. Recalling that $G_{xx} = G_{xx}^H$, it is possible to write

$$G_{xx}(\omega_i) = U^i \Sigma^i U^{iH} \quad (11)$$

where $U^i \in \mathbb{C}^{N_o \times N_o} = [u^{i(1)}, \dots, u^{i(N_o)}]$ and $\Sigma^i \in \mathbb{R}^{+N_o \times N_o}$ are the matrix of the N_o left singular vectors and the diagonal matrix of the singular values (σ_j^i , $j = 1, \dots, N_o$), respectively, associated to the i -th spectral line. If the considered frequency line is practically coincident with the k -th natural frequency, ω_{nk} , then the SVD of $G_{xx}(\omega_{nk})$ will return a predominant singular value, σ_p^k , since the rank of $G_{xx}(\omega_{nk})$ is unitary due to the hypothesis of SDOF system behavior around the peak of resonance. It is worthwhile to observe that p is generally set to one by the common numerical routines. Moreover, it is possible to estimate the corresponding k -th mode shape, $\psi^{(k)}$, from the corresponding p -th left vector, $u^{k(p)}$. Specifically, when $\omega_i = \omega_{nk}$, Eqs. (10) and (11) yield to the following approximation:

$$\psi^{(k)} = u^{k(p)} \quad (12)$$

Therefore, the procedure for the estimate of the natural frequencies and mode shapes will perform an initial SVD of the $(N/2) + 1$ spectral density matrices. The natural frequencies of the system will be estimated from those frequencies to which the singular values σ_p^k exhibit their local maxima, whereas the corresponding p -th left vector, $u^{k(p)}$, give an estimate of the k -th mode shape. Although these modal parameters are estimated in the frequency domain, the identification of the damping ratios requires a time domain technique, i.e., the logarithmic decrement, Ref. [1], performed on the SDOF auto correlation functions. Such functions are achieved by filtering the auto spectral density functions with an ideal band-pass filter, centered on the natural frequency of the mode of interest, and performing the inverse FFT in order to obtain the typical free-decay functions.

2.2. Mode shape scaling technique

Unfortunately, the output only techniques do not allow to estimate the generalized parameters, such as the generalized masses, because the excitation force is unknown. As a result, the mode shapes obtained so far, generally called “operational mode shapes”, remain unscaled, restricting then the applicability of the operational modal models. In the following, a procedure to obtain the generalized parameters, based on the works presented in Refs. [5,7,8], is outlined. If the reference structural model, expressed by its stiffness (K) and mass (M) matrices, is perturbed with a change of its stiffness, ΔK , and

mass, ΔM , properties, the undamped eigenvalue problem, written for the k -th eigenvalue, $\omega_{n_k}^2$, with the corresponding not normalized eigenvector $\psi^{(k)}$, is

$$(K + \Delta K)(\psi^{(k)} + \Delta\psi^{(k)}) = (M + \Delta M)(\psi^{(k)} + \Delta\psi^{(k)})(\omega_{n_k}^2 + \Delta\omega_{n_k}^2) \quad (13)$$

in which the new values of the k -th eigenfrequency, $\bar{\omega}_{n_k}^2$, and eigenvector, $\bar{\psi}^{(k)}$ are expressed as $\bar{\omega}_{n_k}^2 = \omega_{n_k}^2 + \Delta\omega_{n_k}^2$ and $\bar{\psi}^{(k)} = \psi^{(k)} + \Delta\psi^{(k)}$. Pre-multiplying the above Eq. (13) by $\psi^{(k)\top}$, neglecting higher order terms, and assuming that the perturbation in the properties of the structure does not affect the mode shapes, one gets

$$\psi^{(k)\top} M \psi^{(k)} \Delta\omega_{n_k}^2 = \psi^{(k)\top} \Delta K \psi^{(k)} - \omega_{n_k}^2 \psi^{(k)\top} \Delta M \psi^{(k)} \quad (14)$$

Finally, considering that, by definition, the k -th generalized mass is given by $m_k := \psi^{(k)\top} M \psi^{(k)}$, Eq. (14) yields

$$m_k = \psi^{(k)\top} M \psi^{(k)} = \frac{\psi^{(k)\top} \Delta K \psi^{(k)} - \omega_{n_k}^2 \psi^{(k)\top} \Delta M \psi^{(k)}}{\Delta\omega_{n_k}^2} \quad (15)$$

Then, k -th scaled eigenvector, $\phi^{(k)}$, can be obtained by performing:

$$\phi^{(k)} = \sqrt{\frac{1}{m_k}} \psi^{(k)} \quad (16)$$

The above Eq. (15) represents a practical first order approximation for the sensitivity of the natural frequencies for light damped structures. In the following section, the scaling procedure of the k -th operational mode shape has been performed considering a mass change only. In this case, by adding small known masses at selected degrees of freedom, *DOFs*, the changes in the poles of the system, $\Delta\omega_{n_k}^2$, could be experimentally evaluated. Therefore, the scaling factors, $\sqrt{1/m_k}$, are easily achieved from Eq. (15) by evaluating the diagonal matrix of the added mass, ΔM and assuming $\Delta K = 0$. It is worthwhile to remark that the accuracy of the approach depends on the amount of the added mass that should be small enough and located so that to comply with the first order approximation hypothesis. Furthermore, the added masses should not be placed near the nodes of the mode shapes in order to reduce the uncertainties in the estimate of the pole shifts. When the mass changes produce small changes of the values of the natural frequencies, the scaling factors, m_k , predicted by Eq. (15) (with $\Delta K = 0$), may be inaccurate. In order to improve such accuracy, the following first order approximation could be used:

$$m_k = -\frac{1}{2\Delta\omega_{n_k}} \psi^{(k)\top} \Delta M \psi^{(k)} \quad (17)$$

in which $\Delta\omega_{n_k} = \bar{\omega}_{n_k} - \omega_{n_k}$. Finally, the FRF matrix could be evaluated from the estimated modal model following the standard formulation, as reported in the previous Eq. (6). If the viscous damping is considered, then the ij -th element of the FRF matrix is synthesized by the following well-known relationship:

$$H_{ij}(\omega) = \sum_{k=1}^M \frac{\phi_i^{(k)} \phi_j^{(k)}}{\omega_{n_k}^2 - \omega^2 + j2\omega\omega_{n_k}\zeta_k} \quad (18)$$

3. Experimental investigation

In this section, the proposed approach, will be investigated through experimental investigations. First, the modal parameters of the reference structure, i.e., natural frequencies, damping ratios, and unscaled mode shapes, will be estimated from the response data, then the effects of the mass loading in predicting the generalized masses will be analyzed. Finally, the comparison between the FRFs evaluated from the output only approach and the ones estimated from the modal model achieved by the traditional input/output analysis, will be presented. Among the several experimental tests that have been carried out to validate the approach, only the findings pertinent to the beam and a plate structures will be outlined for brevity. Nevertheless, they are of general validity giving guidelines that could be followed by a wide range of applications.

3.1. Beam structure

The experimental analysis was performed on a cantilever aluminum beam of dimensions $0.2 \times 0.0154 \times 0.00285$ m, Ref. [11]. The considered experimental degrees of freedom were the vertical translations of the beam measured at four equally spaced locations along the span (numbered starting from the clamped end). The response of the structure, randomly excited with a “pencil” crawling on one side of the beam, was recorded in the period of 40.96 s, Fig. 1, and the auto and cross spectral densities, considered in a 0–400 Hz frequency band, were evaluated using 16 data block records of length of 2048 sampling points. Once the spectral density matrix was evaluated, the analysis of the corresponding singular values was

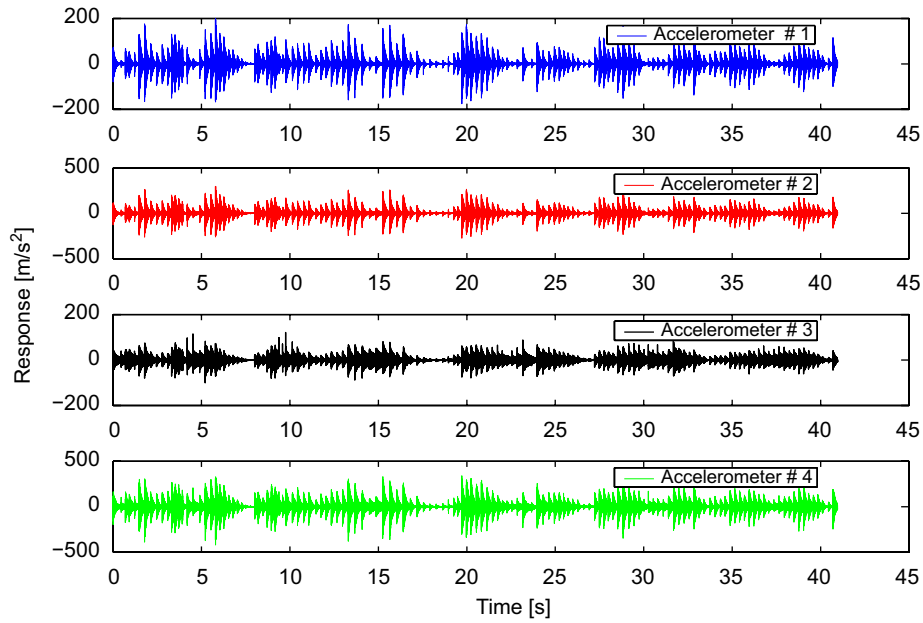


Fig. 1. Time responses of the beam structure.

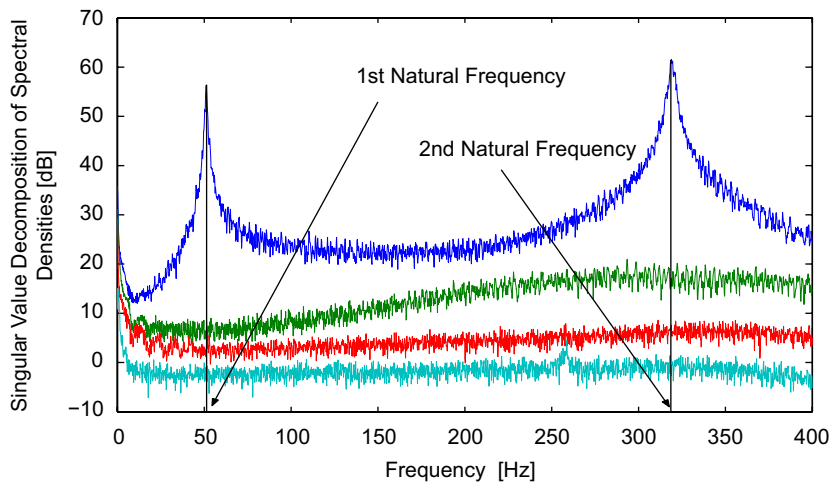


Fig. 2. Estimate of the natural frequencies of the beam structure with FDD technique.

Table 1

Natural frequencies, f_n , and damping ratios, ζ_n , of the beam structure estimated by the output only experimental modal analysis

Mode #	f_n (Hz)	ζ_n (%)
1	51.18	0.49
2	318.83	0.25

performed for all the frequencies considered in the experimental investigation, as reported in Fig. 2. From this analysis, two eigenvalues were clearly identified from the frequencies where the singular values exhibited their (local) maxima, accordingly with the theoretical prediction. Also the identified mode shapes (not reported) are in excellent agreement with the theoretical ones. The estimated natural frequencies and damping ratios (these last ones evaluated in time domain using the logarithmic decrement approach) are reported in Table 1. Furthermore, the effects of the added mass on the estimate of

Table 2
Eigenfrequency shifts due to mass loading for the beam structure

Test #	f_{n1} (Hz)	ε_1 (%)	f_{n2} (Hz)	ε_2 (%)
1	50.01	1.90	310.62	2.34
2	50.40	1.14	316.68	0.44
3	49.23	3.43	305.15	4.06
4	48.45	4.96	303.39	4.62

Table 3
Generalized masses of the beam structure

Mode #	Test #1	Test #2	Test #3	Test #4
1	0.0057	0.0050	0.0047	0.0047
2	0.0050	0.0061	0.0050	0.0052

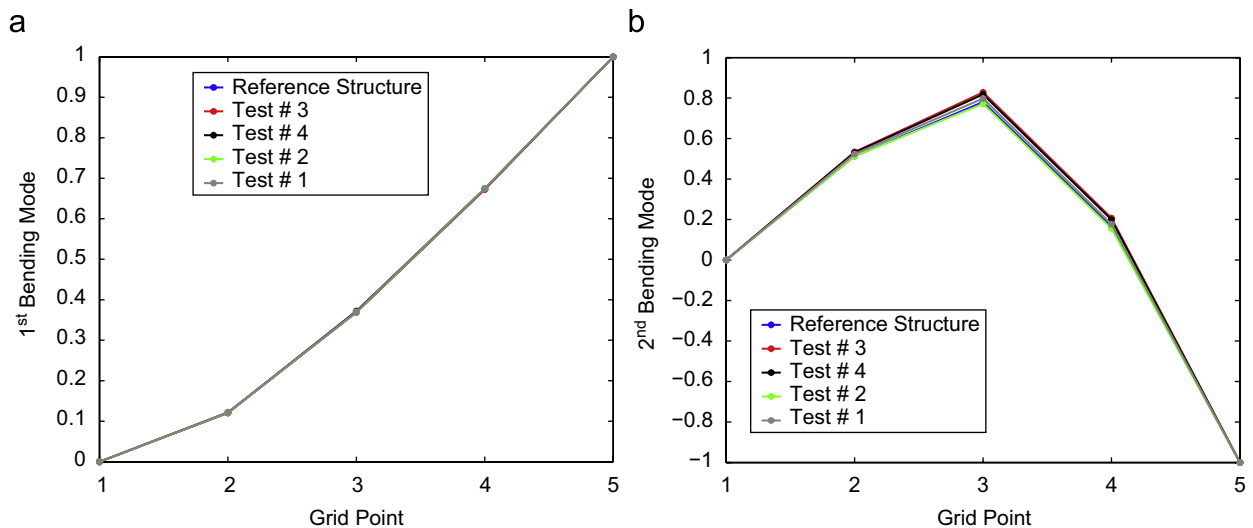


Fig. 3. Effects of the mass loading on the beam structure. (a) Effect of mass loading on the first eigenvector. (b) Effect of mass loading on the second eigenvector.

the generalized parameters were considered. Four additional experimental tests were performed in which different mass loadings of the structure were considered. Specifically, in Test #1, four masses of 0.27 g were placed at the four experimental degrees of freedom; in Test #2, two masses of 0.54 g were placed at the first and third experimental point; Test #3 used the same masses as the previous one, but located at second and fourth experimental point. Finally, the Test #4 used four masses of 0.54 g located in all the experimental points. The generalized masses were computed from the knowledge of the mass changes and from the measure of the eigenfrequency shifts, as prescribed by Eq. (15). These last shifts are reported in Table 2, where ε_1 and ε_2 refer to the measured change, in percentage, corresponding to the first and second mode, respectively. The resulting scaling factors are reported in Table 3, whereas the comparison of the resulting mode shapes with the corresponding achieved for the reference structure is shown in Fig. 3 for the first and second modes, respectively. All the performed additional tests introduced no remarkable modification to the dynamical behavior of the structure, i.e., the mode shapes are practically unchanged, and the eigenfrequency shifts do not exceed the quota of 5% drift. The accuracy of the process for the estimate of the generalized mass could be evaluated recalling the orthogonality properties of the modal base with respect to the mass distribution. For all the identified k -th modes, the distance, δ , between the theoretical unit value of the double product $\phi^{(k)T} M \phi^{(k)}$ and the actual one, could be used as a criteria to be followed for an optimal mass placement, when evaluating the scaling factors. In addition, the zero value of the cross product $\phi^{(h)T} M \phi^{(k)}$ should be checked for completeness. Introducing the mass matrix of the beam structure under investigation, with the aid of an updated finite element model, it was possible to evaluate such distances that are reported, in percentage, in Table 4 for the two identified mode shapes and for the four different tests. These distances seem to depend on the total value of the added mass itself as well as on the order of the mode. Furthermore, a dependency on how the

Table 4
Effects of mass loading in the normalization procedure of the eigenvectors of the beam structure

Mode #	δ (%) ($= 1 - \phi^{(k)\top} M \phi^{(k)}$)			
	Test #1	Test #2	Test #3	Test #4
1	15.17	4.12	-3.18	-3.83
2	-1.51	15.50	-2.57	1.08

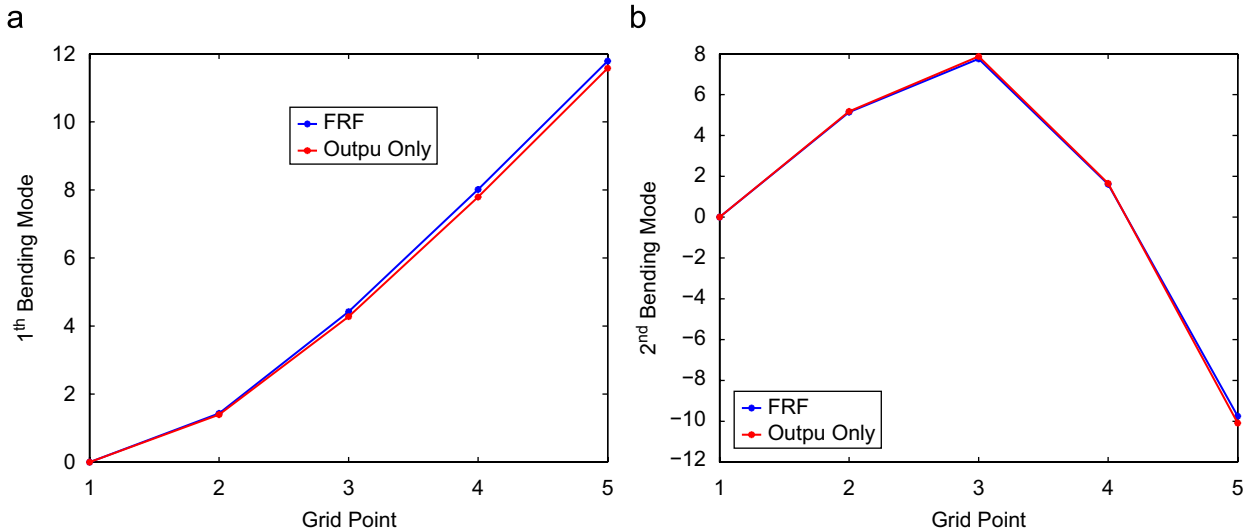


Fig. 4. Comparison between the eigenvectors (unitary mass scaling) of the beam structure: (a) first eigenvector and (b) second eigenvector.

added mass is distributed on the structure is reported. Specifically, the mass distribution of Test #1 resulted in a very poor identification of the generalized masses for the first eigenmode, probably due to the lack of accuracy in determining the change in the natural frequencies. Test #2 had the worst deviation from unitary value and nonzero values of some cross products have been noticed. Test #3, although with low errors, reported nonzero values of the cross products as the previous test. The mass distribution of Test #4 had the lowest errors in the normalization conditions, with scaled eigenmodes practically the same of those estimated from *FRF* achieved with the input/output analysis (for this case, a least square residue/pole polynomial ratio fitting has been adopted), as shown in Fig. 4 for the first and second mode shape, respectively. The complete *FRF* matrix can be achieved considering Eq. (18) and by using the estimated poles and the normalized eigenvectors. In Figs. 5, 6 one of the available columns of the *FRF* matrix is depicted. In each picture, the *FRFs* synthesized with the modal parameters obtained both with the standard input/output analysis (synthesized) and with the output only analysis (synthesized from output only) are compared with the one achieved with the standard H_2 input/output approach (measured), Ref. [15], confirming the correctness of the estimate performed with the proposed procedure around the peak of resonance.

3.2. Plate structure

The dynamic behavior of a composite plate, used in a space application as described in Ref. [13], is further investigated. The structure is considered under free-free boundary conditions (provided by suspending it with proper elastic bands, as shown in Fig. 7), whereas the frequency band of interest was 0–3200 Hz. The acquisition time was 2.56 s, and 2^{14} sampling points were used. An overlap of 90% of the data blocks of 2048 spectral lines is also introduced to reduce the effects of the nondeterministic components of the output signals. The time responses of 64 experimental degrees of freedom, uniformly distributed over the composite plate, Fig. 8a, were measured by five roving accelerometers. A crawling pencil provided the white noise excitation of the structure, as reported in Fig. 8b where the time histories corresponding to the first set of five accelerometers are reported. The natural frequencies of the composite structure were estimated from the analysis of the maximum values of the singular values as a function of the frequency line. This *peak-picking* technique led to the singular value diagram reported in Fig. 9. As in the previous subsection, the unscaled mode shape was estimated from the singular vector corresponding to the maximum singular value, whereas the damping ratios were achieved in time domain from the

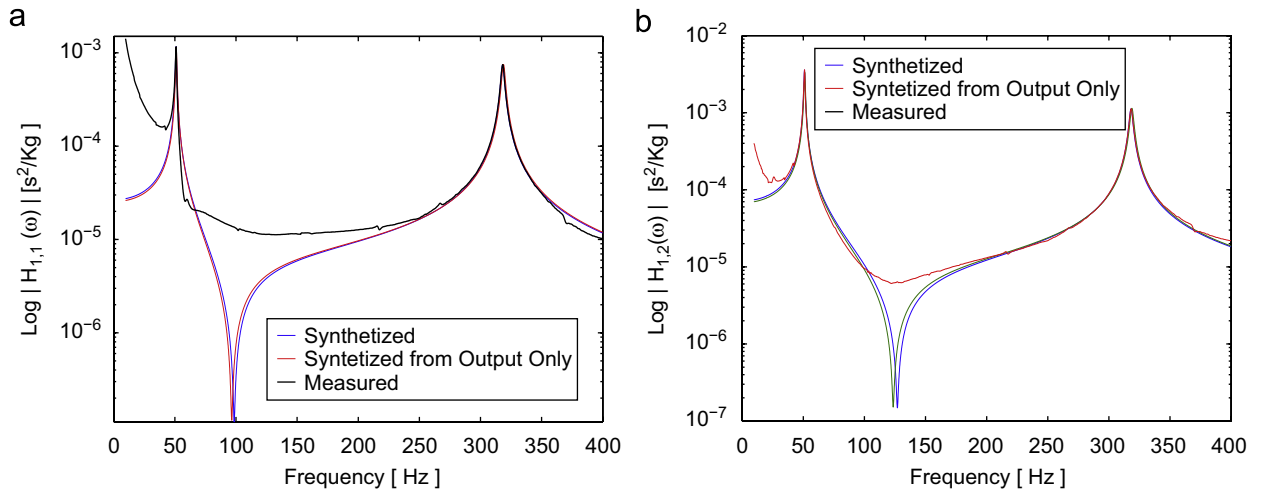


Fig. 5. Comparison between the frequency response functions of the beam structure—(a) $H_{11}(\omega)$, (b) $H_{21}(\omega)$.

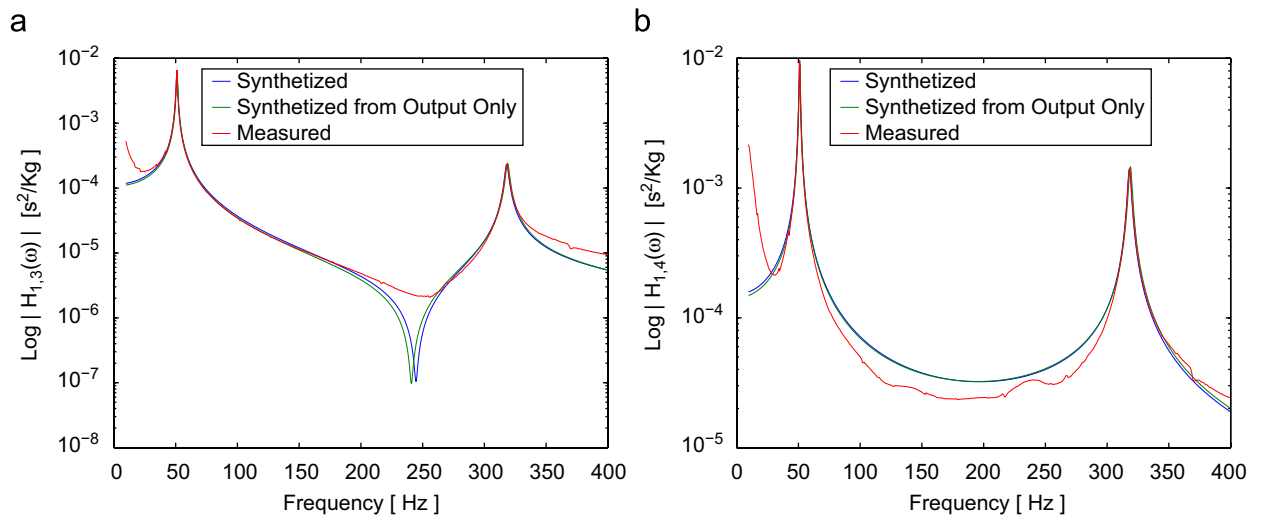


Fig. 6. Comparison between the frequency response functions of the beam structure—(a) $H_{31}(\omega)$, (b) $H_{41}(\omega)$.

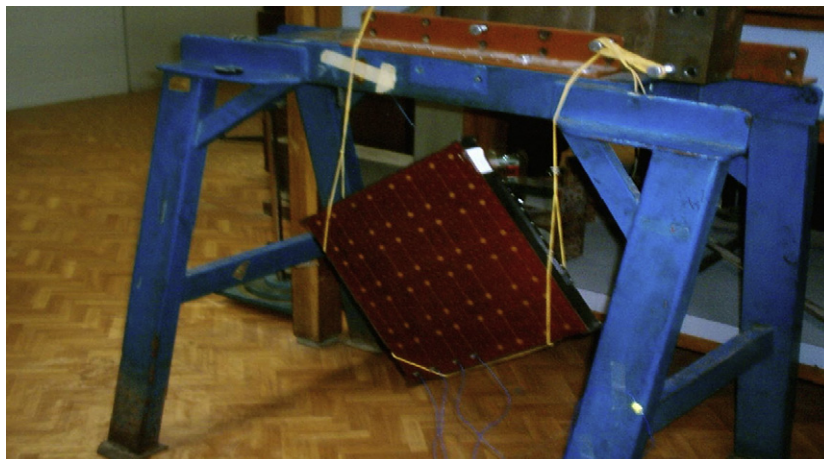


Fig. 7. Experimental setup of the composite plate.

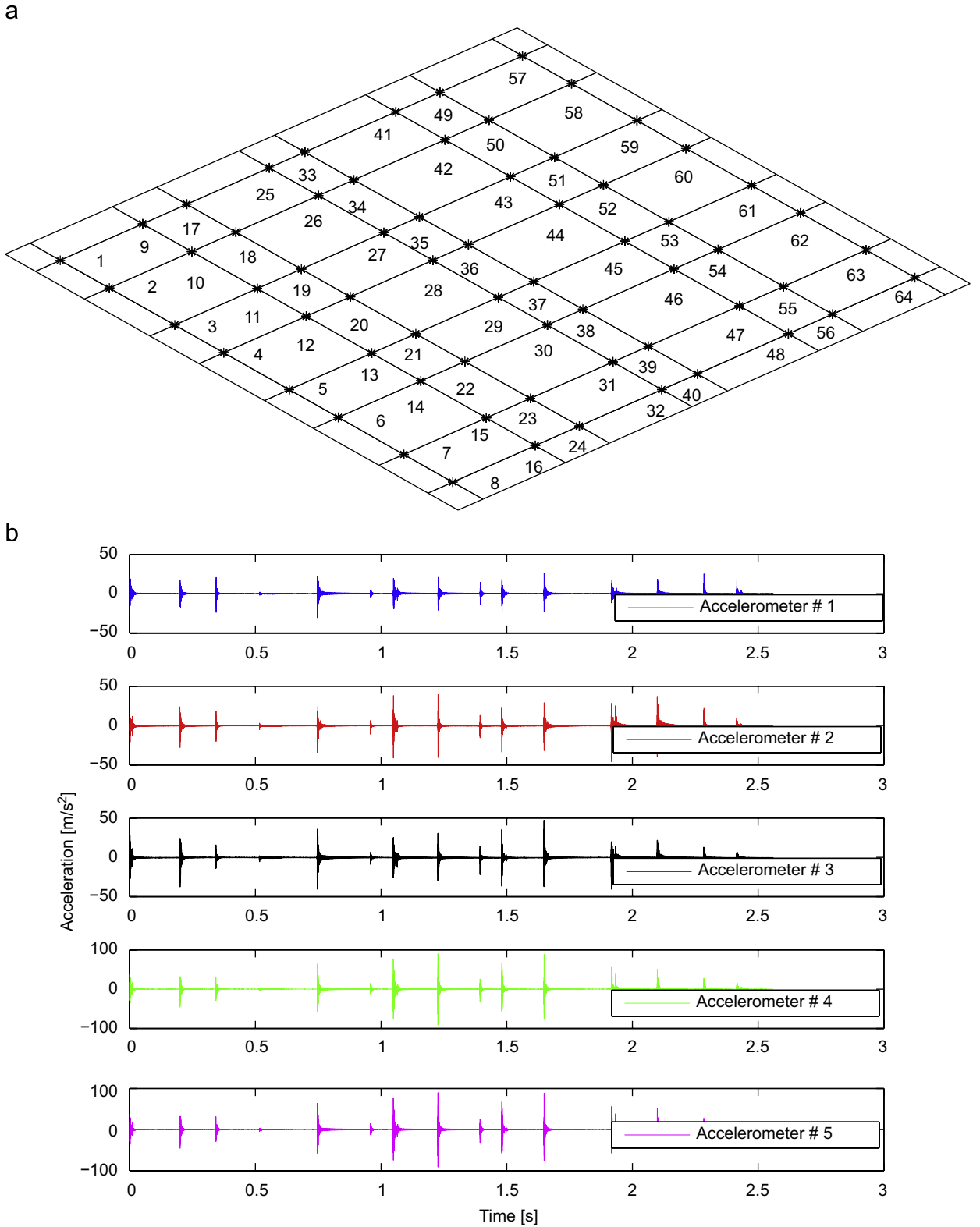


Fig. 8. Measurement of the responses: (a) Position of the measurement points. (b) Time histories of the acceleration output—roving #1.

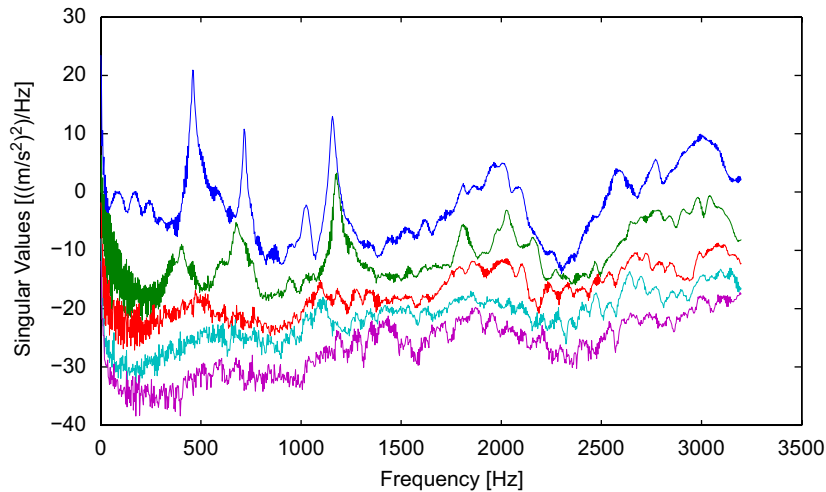


Fig. 9. Estimate of the natural frequencies of the composite plate with FDD Technique.

Table 5

Natural frequencies, f_n , and damping ratios, ζ_n , of the plate structure estimated by the output only experimental modal analysis

Mode #	f_n (Hz)	ζ_n (%)
1	461.75	0.71
2	718.71	0.58
3	1024.90	1.80
4	1175.80	0.80

Table 6

Mass loading of the composite plate for each of the performed tests

Test #	ΔM (kg)	Grid number
1	0.10	11, 14, 17, 24, 29, 36, 41, 48, 51, 54
2	0.10	3, 6, 17, 24, 29, 36, 41, 48, 59, 62
3	0.14	1, 3, 6, 8, 17, 24, 29, 36, 41, 48, 57, 59, 62, 64
4	0.08	3, 17, 24, 29, 36, 41, 48, 62

SDOF free decay using the logarithmic decrement technique. Both the estimated natural frequencies and damping ratios are reported in Table 5. It is worthwhile to remark that the modal identification of the output only procedure is perfectly compatible with the one achieved by other input/output techniques, as reported in Ref. [13]. Again, the first step in the identification process of the generalized masses was to perform one more modal survey on the reference plate with a known increase of the mass distribution. In order to evaluate the effects of different mass loading on the estimate of the scaling factors, four different tests were performed. The mass distribution was changed so that the natural frequency shifts were about 5%, average, with negligible changes in the mode shapes. The resulting mass distribution adopted for each test is reported in Table 6, in which the grid numbers refer to Fig. 8a, whereas the total mass increase was achieved using 0.01 kg lumped masses placed at each grid point. The resulting natural frequencies and corresponding shifts, for each of the performed test, are summarized in Table 7. As final step, all of the four tests were used to estimate the modal masses. The accuracy of such estimates was evaluated following the approach developed when dealing with the beam structure. From this analysis, it seemed that the evaluation of the modal masses using the mass changes of Test #2 was the most accurate with respect to the ones derived from the other tests. Indeed, the added mass for this test concerned a wider area of the plate structure, with respect to Test #1, whereas the eigenfrequency shifts corresponding to Test #3 and Test #4 are either to large or to small, respectively. The resulting modal masses are reported in Table 8. From the estimates of the natural frequencies, damping ratios, mode shapes, and modal masses, the response model, i.e., the whole FRF matrix, could be

Table 7
Natural frequency shifts due to the mass loading of the composite plate

Mode #	Test #1 (Hz)	Δf_n (%)	Test #2 (Hz)	Δf_n (%)
1	447.09	2.72	443.97	3.40
2	684.71	4.37	672.20	6.11
3	922.33	10.06	931.70	9.15
4	1125.50	4.51	1122.40	4.78
	Test #3 (Hz)	Δf_n (%)	Test #4 (Hz)	Δf_n (%)
1	415.83	9.52	450.22	2.04
2	669.08	6.55	681.58	4.80
3	906.69	11.59	934.83	8.84
4	1075.50	8.76	1147.40	2.66

Table 8
Estimate of the modal masses of the composite plate from Test #2

Mode #	Modal mass
1	2.88
2	6.09
3	0.35
4	4.27

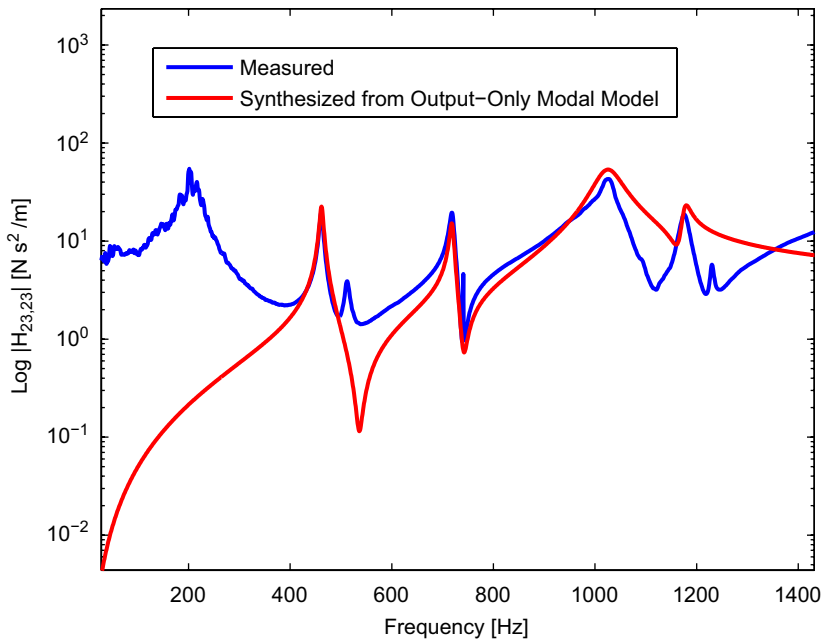


Fig. 10. Comparison among the FRFs of the composite plate.

finally synthesized from Eq. (18). In Fig. 10 a comparison between the measured and synthesized, from output only data, FRFs is depicted considering, for example the driving point corresponding to the grid number 23. From this picture, a perfect identification of the FRF is acknowledged except for the third natural frequency where a small reduction of accuracy is evident. For this specific mode, the assumption that there are no changes in the modal shapes after the structural modification was not fully accomplished. Although the mass loading corresponding to Test #2 had no practical influence on the first, the second, and the fourth modal shapes, the third one exhibited an evident modification. Comparing such a mode

with the corresponding of the original structure, a modal assurance criterion, MAC, value as low as about 70% was computed, whereas a relative high frequency shift, about 10%, was measured, as reported in Table 7. A possible explanation of this behavior could be addressed to the type of this third mode. This is a typical “drum” mode, strongly affected by the location of the added mass, especially by those located in the proximity of the center of the plate, i.e., grid numbers 29 and 36. The consequence of this mass loading was a significant modification of the nodal line, with respect to the corresponding perturbation that could be observed in the other modes.

4. Concluding remarks

In this paper, an approach devoted to the estimate of the generalized parameters of a vibrating structure using “output only” data has been investigated. This approach requires some additive experimental tests by perturbing the original structure with some known changes in mass distribution (or more in general in stiffness distribution). At least the measure of two time responses are needed to evaluate the modal parameters and, in turn, the whole frequency response function matrix could be easily achieved with a significant level of precision. In particular the experimental results showed an appealing comparison between the measured FRFs (by a classical input/output approach) and those derived by the output only modal testing. Moreover, the effects of the entity and distribution of the perturbation mass have been investigated considering both a cantilever aluminum beam and a free-free composite plate. As a result of this investigation, a criteria for the mass loading has been outlined. It seems that it is preferable to uniformly distribute the added mass across the structure, so that to avoid the mass loading corresponding to a node of a generic mode. Furthermore, it seems convenient to perturbate the structure so that natural frequency shifts are large enough to reduce the errors in their estimates, say 5%, keeping the mode shapes practically unchanged. Finally, the frequency domain decomposition technique, used to estimate the modal parameters, seems to be a reliable and efficient estimator for the natural frequency and mode shapes. These results confirm the interest given to the output-only techniques. In fact, they merge experimental efficiency (due to the low cost required to run the experimental activities since no input measurements are needed) with the possibility to get all the necessary data in order to achieve a complete dynamic identification of a structure.

Acknowledgments

This paper has been partially supported by the grant Università degli Studi di Roma “La Sapienza”—Ateneo 2001: “Progettazione Integrata Aeronautica”. I wish to thank Prof. Rune Brincker for inspiring this work. The useful comments and discussions with Prof. A. Agneni, Prof. L. Balis Crema, and Prof. F. Mastroddi (in strictly alphabetical order) are gratefully acknowledged.

References

- [1] D.J. Ewins, Modal Testing: Theory and Practice, Research Studies Press Ltd., Tauton, Somerset, England, January 1995.
- [2] R. Brincker, C.E. Ventura, P. Andersen, Why output-only modal testing is a desirable tool for a wide range of practical applications, XXI IMAC 3–6 February, Orlando, FL, USA, 2003, pp. 265–272.
- [3] H. Van der Auweraer, L. Hermans, B. Dierckx, J. Deweer, In-operation modal analysis: theory and application, Course of Modal Analysis: Theory and Practice, K.U. Leuven, Belgium, September 11–12, 2000.
- [4] A. Agneni, L. Balis Crema, G. Coppotelli, Time and frequency domain modal parameter estimation by output-only functions, International Forum on Aeroelasticity and Structural Dynamics, 04–06 June, Amsterdam, NL, 2003.
- [5] R. Brincker, P. Andersen, A way of getting scaled mode shapes in output only modal testing, XXI IMAC, 3–6 February, Orlando, FL, USA, 2003, pp. 141–145.
- [6] A. Sestieri, W. D'Ambrogio, Frequency response function versus output-only modal, testing identification, XXI IMAC, 3–6 February, Orlando, FL, USA, 2003, pp. 11–46.
- [7] E. Parloo, P. Verboven, P. Guillaume, M. Van Overmeire, Sensitivity-based operational mode shape normalization, MSSP, (073) 2001.
- [8] G. De Vries, Sondage des Systemes Vibrantes par Masses Additionnelles, La Recherche Aeronatique, vol. 30, Paris, France, 1952, pp. 47–49.
- [9] R. Brincker, L. Zhang, P. Andersen, Modal identification from ambient responses using frequency domain decomposition, XVIII IMAC, 07–10 February, San Antonio, TX, USA, 2000.
- [10] L. Balis Crema, G. Coppotelli, Output-only approach for finite element model updating of AB-204 helicopter blade, in: Proceedings of 46-th AIAA Structures, Structural Dynamics, and Materials Conference, Austin, TX, USA, paper no. AIAA-2005-2249, April 18–21, 2005.
- [11] G. Coppotelli, Identification of frequency response functions by “output-only” experimental data, in: Proceedings of XVII Associazione Italiana di Aeronautica e Astronautica, Rome, I, 2003.
- [12] A. Agneni, R. Brincker, G. Coppotelli, On modal parameter estimates from ambient vibration tests, in: International Conference on Noise and Vibration Engineering, Leuven, Belgium, 2004, pp. 2239–2248.
- [13] G. Coppotelli, L. Balis Crema, Estimates of FRFs from Output-only data of a space mission payload component, in: Proceedings of 47th AIAA/ASME/ASCE/AHS/ASC Structures, Structural Dynamics, and Material Conference, Newport, RI, USA, paper no. AIAA-2006-1887, May 1–4, 2006.
- [14] J.S. Bendat, A. Piersol, Random Data, Wiley, New York, 1986.
- [15] W. Heylen, S. Lammen, P. Sas, Modal Analysis Theory and Testing, Department of Mechanical Engineering, K.U. Leuven, Leuven Belgium, 1997.